Structural Engineering and Mechanics, Vol. 9, No. 5 (2000) 433-448
DOI: http://dx.doi.org/10.12989/sem.2000.9.5.433

Serendipity and bubble plus hierarchic finite elements for thin to thick plates

Lucia Della Croce† and Terenzio Scapolla‡

Dipartimento di Matematica, Università di Pavia, I-27100 Pavia, Italy

Abstract. In this paper we deal with the numerical solution of the Reissner-Mindlin plate problem with the use of high order finite elements. In previous papers we have solved the problem using approximation spaces of Serendipity type, in order to minimize the number of internal degrees of freedom. Since further numerical experiences have evidenced that the addition of bubble functions improved the quality of the results we have modified the previous family of hierarchic finite elements, adding internal degrees of freedom, to make a systematic analysis of their performance. Of course, more degrees of freedom are introduced. Nonetheless the numerical results indicate that the reduction of the error outnumbers the increase of degrees of freedom and therefore bubble plus elements are preferable.

Key words: Reissner-Mindlin plate; conforming hierarchic finite elements; bubble functions.

1. Introduction

The so-called Reissner-Mindlin plate describes the deformation of a plate subject to a transverse loading when transverse shear deformation is taken into account. According to the model fibers normal to the undeformed middle surface remain on a straight line which is not necessarily normal to the deformed middle surface. The model, in its formulation, involves the transverse displacement of the midplane and the rotation of fibers normal to the midplane. The variational setting makes use only of first derivatives. For this reason continuous functions ensure a conforming approximation. Despite its simple approach the discretization of the Reissner-Mindlin model is not straightforward. The inclusion of transverse shear strain effect in standard finite element models introduces undesirable numerical effects. The approximate solution is very sensitive to the plate thickness and, for small thickness, it is very far from the true solution. The phenomenon is known as locking of the numerical solution. As the plate thickness becomes small the Reissner-Mindlin model enforces the Kirchhoff constraint that the rotation equals the gradient of the displacement. At the continuous level this means that the solution of the Reissner-Mindlin model converges to the solution of a biharmonic problem. At the discrete level the Kirchhoff constraint is imposed on the finite element subspaces in the limit.

Standard low order finite elements are not able to meet the Kirchhoff constraint and therefore are subject to the locking phenomenon. The most common way to avoiding the locking problem is to modify the variational formulation in order to enforce a weaker discrete Kirchhoff condition (see, e.g., the MITC formulation (Bathe 1982, Brezzi *et al.* 1991, Della Croce *et al.* 1995)). In previous papers

† Professor
‡ Professor

(Della Croce *et al.* 1992) we have dealt with the Reissner-Mindlin problem combining its *plain* formulation with the use of *hierarchic high order* finite elements. The locking phenomenon was strongly reduced and the numerical performances were quite effective for all practical values of thickness. However, analyzing the behavior for $t \to 0$, it appeared that locking was still present. To keep low the number of degrees of freedom we used finite elements of Serendipity type, where the number of internal shape functions is highly reduced. A natural idea is to test *complete* finite elements, i.e., elements using complete polynomial approximation spaces, for comparing their performances against Serendipity elements. Such a problem has been recently addressed and carefully analyzed by Babuška and Elman (1993) in the framework of the so-called *h-p* version of the finite element method. We focus our attention on the performances of the finite elements applied to the Reissner-Mindlin plate problem. Due to the hierarchic structure the implementation of the new elements has required only minor modifications of the previous program. Two main results have been achieved. First, a remarkable improvement of the quality of the results; when cost versus accuracy is considered, complete elements are more convenient: the gain in convergence outnumbers the increase of cost due to the larger number of degrees of freedom. Second, from the value p=3 onwards the elements exhibit a weaker form of locking. The reason is due to the fact that the corresponding approximation spaces are "enough rich", in a sense that will be explained on a mathematical basis, to overcome the numerical misbehavior and produce satisfactory results.

The outline of the paper is the following. In Section 2 we recall the Reissner-Mindlin model for plate problems. In Section 3 we describe the finite elements approximation and introduce the new hierarchic finite elements. In Section 4 we deal with the discrete problem. Finally, several numerical results are reported.

2. The Reissner-Mindlin assumptions for the plate problem

Hereafter we shortly recall the problem. Details can be found, e.g., in Zienkiewicz (1991). We consider the Reissner-Mindlin assumptions for the plate bending problem. This plate theory takes into account the transverse shear deformations. The theory uses the hypothesis that particles of the plate originally on a line that is normal to the undeformed middle surface remain on a straight line during deformation, but this line is not necessarily normal to the deformed middle surface. The so-called *in plane* displacements u, v and the normal displacement w have the form

$$\begin{aligned} u(x, y, z) &= z\psi_x(x, y) \\ v(x, y, z) &= z\psi_y(x, y) \\ w(x, y, z) &= v(x, y) \end{aligned} \tag{1}$$

The functions ψ_x and ψ_y are the rotations of the normal to the undeformed middle surface in the x-z and y-z planes, respectively. The strain energy U can be written in the two components U_b and U_s, representing the bending and shear contribution to the energy, respectively. Setting $U=U_b+U_s$ we have

$$U_b=\frac{Et^3}{24(1-\nu^2)}\int_\Omega \left\{ \psi_{x/x}^2 + \psi_{y/y}^2 + 2\nu\psi_{x/x}\psi_{y/y} + \frac{1-\nu}{2}(\psi_{y/x} + \psi_{x/y})^2 \right\} dxdy \tag{2}$$

$$U_s=\frac{Etk}{4(1+\nu)}\int_\Omega \{(v/x + \psi_x)^2 + (v/y + \psi_y)^2\} dxdy \tag{3}$$

In the previous relations Ω denotes the domain of the plate, E the Young's modulus, t the thickness of the plate, ν the Poisson's ratio, k the shear correction factor (usually taken as 5/6). The solution of the problem requires the potential energy to be stationary, i.e., the functional $U=U(\psi_x, \psi_y, v)$ attains its minimum. Taking into account the contribution of the external load $f(x, y)$, after scaling, normalizing some physical constant and setting $\vec{\phi}=(\phi_x, \phi_y)$, $\vec{\psi}=(\psi_x, \psi_y)$ the problem can be stated as:

$$\begin{cases} \text{Find}(\vec{\phi}, w) \in \Psi \times V \text{ satisfying} \\ J(\vec{\phi}, w) = \min\limits_{(\vec{\psi}, v) \in \Psi \times V} J(\vec{\psi}, v) \end{cases} \tag{4}$$

where $J(\vec{\psi}, v)$ is of the form

$$J(\vec{\psi}, v) = \frac{1}{2}A(\vec{\psi}, \vec{\psi}) + \frac{1}{2}t^{-2}\left\| \nabla v - \vec{\psi} \right\| - (f, v)$$

and $A(\vec{\phi}, \vec{\psi})$ is defined as

$$A(\vec{\phi}, \vec{\psi}) = \frac{E}{12(1-\nu^2)}\int_\Omega \{\phi_{x/x}\psi_{x/x} + \phi_{y/y}\psi_{y/y}$$

$$+\nu(\phi_{x/x}\psi_{y/y} + \phi_{y/y}\psi_{x/x}) + \frac{1-\nu}{2}(\phi_{x/y} + \psi_{y/x})(\psi_{x/y} + \psi_{y/x})\}dxdy \tag{5}$$

We consider, for the sake of simplicity, the case of a clamped plate. In this case we have $\Psi=(H_0^1)^2$ and $V= H_0^1$. Setting

$$J_1(\vec{\psi}, v)=\frac{1}{2}A(\vec{\psi}, \vec{\psi}) - (f, v) \tag{6}$$

$$J_2(\vec{\psi}, v)=\frac{1}{2}\left\| \nabla v - \vec{\psi} \right\| \tag{7}$$

$$J(\vec{\psi}, v)=J_1(\vec{\psi}, v) + t^{-2}J_2(\vec{\psi}, v) \tag{8}$$

we are looking for

$$\min_{(\vec{\psi}, v) \in \Psi \times V} J(\vec{\psi}, v)= \min_{(\vec{\psi}, v) \in \Psi \times V} [J_1(\vec{\psi}, v) + t^{-2}J_2(\vec{\psi}, v)] \tag{9}$$

We are interested in finite elements that yield good approximations when the thickness t becomes small. An optimal element is one that is uniformly good for $t \to 0$. The limit problem for $t=0$ can be written as

$$J_1(\vec{\phi}, w)= \min_{\substack{(\vec{\psi}, v) \in \Psi \times V \\ J_2(\vec{\psi}, v)=0}} J_1(\vec{\psi}, v) \tag{10}$$

In the limit case $t=0$ we have $\vec{\phi}=\nabla w$, i.e., the Reissner-Mindlin problem converges to the Kirchhoff problem.

3. Finite element approximation

In Della Croce *et al.* (1992), we have introduced a family of hierarchic finite elements to overcome the locking of the numerical approximation of the Reissner-Mindlin plate. While the common feature of most finite elements proposed by several authors is the low order together with a modified formulation, we have combined the plain formulation with the use of high order finite elements. Although our numerical results indicate that high order elements are able to absorb the locking phenomenon for all thickness of practical interest, we have noticed a relation linking the order of the polynomials used in the approximation and the locking behavior. Since we have used classical Serendipity elements, i.e., elements with the minimum number of internal degrees of freedom (see, e.g., Szabó *et al.* 1991), a natural idea is that of testing the performance of complete finite elements. Hereafter we first briefly illustrate the features of the Serendipity finite elements and then we explain the modifications made to add internal degrees of freedom. Only polynomial functions are used to construct the approximation spaces. The same spaces are used to approximate normal deflection and rotations. The degree of the polynomial spaces varies from one to four. The family is hierarchic, i.e., new shape functions are added to increase the degree of approximation, leaving unchanged the previous functions. The functions used are based on the family of Legendre polynomials to reduce the roundoff error accumulation with respect to the increase of the polynomial degree. Moreover, the orthogonality properties of Legendre polynomials are transferred to the elementary stiffness matrix which has the minimum number of nonvanishing elements. Finite elements of Serendipity type are used in order to minimize the number of internal degrees of freedom. We denote the elements of the family with the names R4, R8, R12, R17, where R stands for *rectangular* element and the number refers the degrees of freedom (of each field).

As previously mentioned, in this work we present a new family of finite elements characterised by the presence of suitable internal functions. These functions are frequently named *bubble functions*, since they vanish along the whole boundary of the finite element and are different from zero only in the interior of the element. The use of bubble functions is known to be rather effective (see, e.g., Babuška *et al.* 1993, Pinsky *et al.* 1989). The aim of this work is to analyze the effect of additional functions and to evaluate the global performance with respect to an accuracy versus cost criterium. We introduce the family of modified elements, named R9, R16, R25, according to the previous convention. We note, on passing, that as an intermediate step we introduce two other elements, denoted by R15, R22. These elements, beside having good convergence properties, have been proved to be useful in the framework of a special mixed formulation (see Della Croce *et al.* 1995, Perugia *et al.* 1997). We observe that the element corresponding to p=1 does not include internal degrees of freedom, since the space of bilinear functions is fully described by four shape functions. Therefore the elements are the same in the old and new family. The family {R4, R9, R16, R25} is still hierarchic, i.e., the stiffness matrices of lower degree are simply the submatrices of the one of higher order. The improved hierarchic elements are obtained by adding internal degrees of freedom to the previous family {R4, R8, R12, R17}. Only the number of internal functions is modified, while nodal and side functions are left unchanged.

Let P_p denote the space of polynomial of degree up to p in each of the two variables. Let S_p be the polynomial spaces of the Serendipity hierarchic shape functions of degree p. Let Q_p be the standard complete space of polynomials of degree p in each of the two variables. Let B_p be the intermediate space, obtained by S_p adding only a limited number of bubble functions. Due to the construction, for a given degree p, the following relation hold between the finite dimensional

Table 1 Total number of shape and bubble functions for the spaces S_p, B_p, Q_p

p	Shape functions			Bubble functions		
	S_p	B_p	Q_p	S_p	B_p	Q_p
1	4	4	4	0	0	0
2	8	9	9	0	1	1
3	12	15	16	0	3	4
4	17	22	25	1	6	9

spaces:

$$P_p \subset S_p \subset B_p \subset Q_p \tag{11}$$

and therefore

$$\dim P_p \leq \dim S_p \leq \dim B_p \leq \dim Q_p \tag{12}$$

In Table 1 the dimensions are given for some values of the degree p. Moreover, the number of internal functions is reported.

For a general value of p the dimension of each space is:

$$\dim S_p = 4p + \frac{1}{2}(p-2)(p-3) \tag{13}$$

$$\dim B_p = \frac{1}{2}p(p+7) = 4p + \frac{1}{2}p(p-1) \tag{14}$$

$$\dim Q_p = (p+1)^2 = 4p + (p-1)^2 \tag{15}$$

To obtain the space B_p we take all monomials of the space S_p and we add the following monomial terms:

$p = 2 : \{x^2y^2\}$;
$p = 3 : \{x^2y^2, x^3y^2, x^2y^3\}$;
$p = 4 : \{x^3y^2, x^2y^3, x^4y^2, x^3y^3, x^2y^4\}$.

A convenient basis for the space Q_p will represent all polynomials made of monomials of degree up to p in each of the two variables x and y. In Table 2 the single monomials terms of the spaces S_p, B_p, Q_p are listed. More precisely, for the standard hierarchic space S_p the monomials are added to increase the degree p. For the spaces B_p and Q_p only the monomials to be added to the correspondent space S_p and B_p, respectively, are listed.

Let us describe the main features of the new elements compared with the old ones. We consider the standard square reference element $[-1, +1]\times[-1, +1]$.

Table 2 Monomial terms of the spaces S_p, B_p, Q_p

p	*Serendipity* space S_p	*Intermediate* space B_p	*Complete* space Q_p
1	$\{1, x, y, xy\}$		
2	$\{x^2, x^2y, xy^2, y^2\}$	$\{x^2y^2\}$	
3	$\{x^3, x^3y, xy^3, y^3\}$	$\{x^2y^2, x^3y^2, x^2y^3\}$	$\{x^3y^3\}$
4	$\{x^4, x^4y, xy^4, y^4, x^2y^2\}$	$\{x^2y^3, x^3y^2, x^3y^3, x^4y^2, x^2y^4\}$	$\{x^3y^4, x^4y^3, x^4y^4\}$

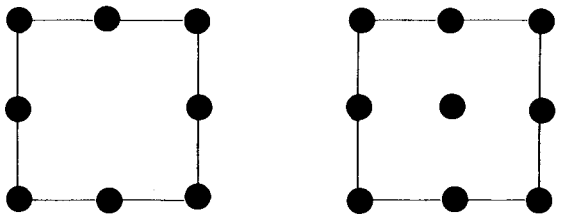

Fig. 1 Serendipity and complete element for p=2

Element R9. The classical Serendipity element of degree two has eight degrees of freedom. The improved element is obtained by adding the sole bubble functions of degree two, i.e., the function

$$b_1(x, y) = (1 - x^2)(1 - y^2) \tag{16}$$

In Fig. 1 both Serendipity and complete element are shown. We recall that for each node three degrees of freedom (one for the displacement and two for the rotations) are present.

Elements R15 and R16. The classical Serendipity element of degree three has twelve degrees of freedom. The improved element is obtained by adding three bubble functions. Since we are dealing with hierarchic elements we keep the previous function and to obtain R15 we add the following functions:

$$b_2(x, y) = x \times b_1(x, y) \tag{17}$$

$$b_3(x, y) = y \times b_1(x, y) \tag{18}$$

In a different way, the bubble functions we have added can be described as the product $P_1 \otimes b_1(x, y)$. Furthermore, by adding the function

$$b_4(x, y) = xy \times b_1(x, y) \tag{19}$$

we get the element R16. In this case the set of bubble functions we add can be described as the product $Q_1 \otimes b_1(x, y)$. In Fig. 2 the elements are shown.

Elements R22 and R25. The classical Serendipity element of degree four has seventeen degrees of freedom and includes the bubble function b_1. Adding five bubble functions we get the element R22. We keep all the previous bubble functions and add:

$$b_5(x, y) = x^2 \times b_1(x, y) \tag{20}$$

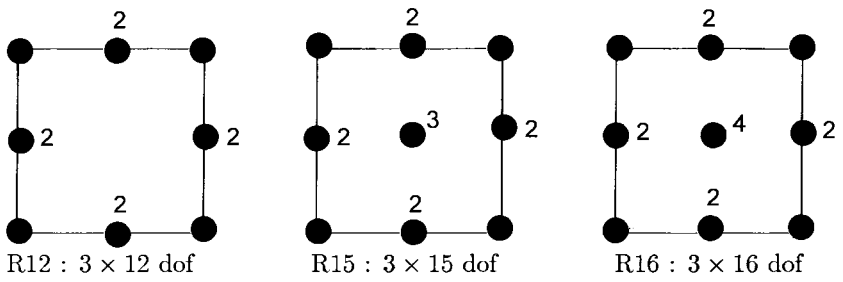

Fig. 2 Serendipity, intermediate and complete

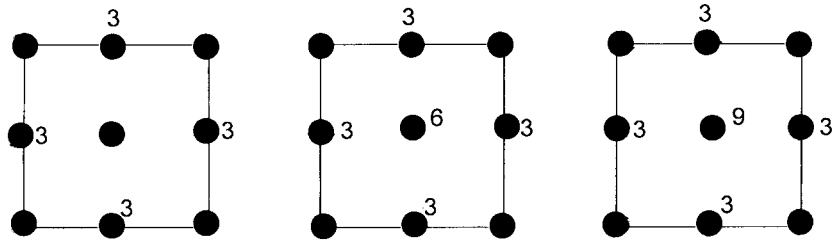

R17 : 3 × 17 dof R22 : 3 × 22 dof R25 : 3 × 25 dof

Fig. 3 Serendipity, intermediate and complete

$$b_6(x, y) = y^2 \times b_1(x, y) \tag{21}$$

The set can be described as the product $P_2 \otimes b_1(x, y)$. Furthermore, by adding the functions

$$b_7(x, y) = x^2 y \times b_1(x, y) \tag{22}$$

$$b_8(x, y) = xy^2 \times b_1(x, y) \tag{23}$$

$$b_9(x, y) = x^2 y^2 \times b_1(x, y) \tag{24}$$

we get the complete element R25. In this case the set of bubble functions can be escribed as $Q_2 \otimes b_1(x, y)$. In Fig. 3 the elements are shown.

4. Discrete problem

Problem in Eq. (4) can be given the following discrete formulation:

$$\begin{cases} \text{Find}(\vec{\phi}_h, w_h) \in \Psi_h \times V_h \text{satisfying} \\ \boldsymbol{J}(\vec{\phi}_h, w_h) = \min\limits_{(\vec{\psi}_h, \upsilon_h) \in \Psi_h \times V_h} \boldsymbol{J}(\vec{\psi}_h, \upsilon_h) \end{cases} \tag{25}$$

where $\boldsymbol{J}(\vec{\psi}_h, \upsilon_h)$ is of the form

$$\boldsymbol{J}(\vec{\psi}_h, \upsilon_h) = \frac{1}{2}\boldsymbol{A}(\vec{\psi}_h, \vec{\psi}_h) + \frac{1}{2}t^{-2}\left\|\nabla \upsilon h - \vec{\upsilon}_h\right\| - (f, \upsilon_h)$$

and the bilinear form $\boldsymbol{A}$ is defined as in (5).

We can write the problem as

$$\boldsymbol{J}_1(\vec{\phi}_h, w_h) = \min_{\substack{(\vec{\psi}_h, \upsilon_h) \in \Psi_h \times V_h \\ \boldsymbol{J}_2(\vec{\psi}_h, \upsilon_h) = 0}} \boldsymbol{J}_1(\vec{\psi}_h, \upsilon_h) \tag{26}$$

with $\boldsymbol{J}_1(\vec{\psi}_h, \upsilon_h)$ and $\boldsymbol{J}_2(\vec{\psi}_h, \upsilon_h)$ defined as in Eqs. (6) and (7).

The previous relation is valid for the limit problem ($t \to 0$). The locking phenomenon, i.e., the degeneration of the numerical solution, is due to the fact that the discrete space

$$K_h = \{(\vec{\psi}_h, v_h) \in \Psi_h \times V_h : \vec{\psi}_h = \nabla v_h\} \tag{27}$$

reduces to the null function. Equivalently, we have locking when

$$\left\| \vec{\psi}_h - \nabla v_h \right\| = 0 \Rightarrow \vec{\psi}_h = \nabla v_h = \vec{0} \tag{28}$$

When the space K_h is "enough rich" then locking can be avoided and error estimates of the following type can be proved:

$$\min_{(\vec{\psi}_h, v_h) \in K_h} [\left\| \vec{\psi} - \vec{\psi}_h \right\|_1 + \| v - v_h \|_1] = O(h^{\alpha}) \tag{29}$$

for some positive constant α.

We show that the element R16 satisfies relation (29) with α=2. Such an estimate is not optimal but nevertheless guarantees a stable numerical behaviour.

Let us denote by Z_h the space corresponding to the finite element introduced by Bogner, Fox and Schmit (see, e.g., Ciarlet 1978). Such a finite element has 16 degrees of freedom and the shape functions are locally represented by the space Q_3, consisting of the polynomials of degree up to three in each of the two variables x and y. The Bogner-Fox-Schmit element is of class C^1. When the space V_h is such that

$$V_h \supset Z_h \tag{30}$$

then, given a function $v \in V$, we can take its interpolated $v^I \in Z_h$. Due to the C^1 continuity the function ∇v^I is of class C^0. Having satisfied the inclusion

$$\Psi_h \supset \nabla Z_h \tag{31}$$

we can take $\vec{\psi}^I = \nabla v^I$, thus having all the pairs $(\vec{\psi}^I, v^I) \in K_h$. We can show that when the spaces V_h and Ψ_h satisfy inclusions (30), (31), and therefore K_h does not reduces to the null function, then the following estimate holds:

$$\min_{(\vec{\psi}_h, v_h) \in K_h} [\left\| \vec{\psi} - \vec{\psi}_h \right\|_1 + \| v - v_h \|_1] = O(h^2) \tag{32}$$

Indeed we have:

$$\min_{(\vec{\psi}_h, v_h) \in K_h} ([\left\| \vec{\psi} - \vec{\psi}_h \right\|_1 + \| v - v_h \|_1] \le [\left\| \vec{\psi} - \vec{\psi}^I \right\|_1 + \| v - v^I \|_1])$$

$$= [\left\| \nabla v - \nabla v^I \right\|_1 + \| v - v^I \|_1] \le \| v - v^I \|_2 \tag{33}$$

and since $v^I \in Z_h \equiv Q_3 \supset P_3$ (32) is proved using the standard interpolation estimate

$$\| v - v^I \|_2 = O(h^2) \tag{34}$$

Let us explain how relations (30)-(31), and therefore the estimate (32), hold for the finite element

R16 giving some more details. The shape functions of the finite element R16 are locally represented by the pace Q_3, i.e., exactly the same space used in the Bogner-Fox-Schmit element. Therefore we have

$$V_h \equiv Z_h \tag{35}$$

In the finite elements we have introduced the same approximation spaces are used for both normal displacement and rotations, and therefore the following relation is satisfied:

$$\Psi_h = V_h \tag{36}$$

Of course, such a choice guarantees that Eq. (31) is satisfied.

5. Numerical results

The following variational formulation has been used for the implementation of the finite elements previously introduced:

$$\begin{cases} \text{Find}(\vec{\phi}_h, w_h) \in \Psi_h \times V_h \text{such that} \\ \dfrac{E}{12(1-\nu^2)}\mathbf{A}(\vec{\phi}_h, \vec{\psi}_h) + \dfrac{Et^{-2}k}{2(1+\nu)}(\nabla w_h - \vec{\phi}_h, \nabla \upsilon_h - \vec{\psi}_h) = (f, \upsilon_h) \ \forall(\vec{\psi}_h, \upsilon_h) \in \Psi_h \times V_h \end{cases} \tag{37}$$

We consider a unit square plate with uniform decomposition in rectangular elements. Due to the symmetry of the domain the computations have been performed on a quarter of plate only. Numerical experiences with distorted decompositions have been carried out using the hierarchic finite elements for shell structures in the Naghdi's model, based on the Reissner-Mindlin assumptions (see Della Croce, Scapolla 1999a and 1999b). It is known that high order finite elements are able to deal with severely distorted decompositions (see Szabó, Babuška 1991).

The plate is subject to the uniform load f=1.0. We take Young's modulus E=3 × 10^6 and Poisson's ratio ν=0.3. Different boundary conditions have been imposed: clamped, soft and hard simply supported.

To compute the integrals appearing in Eq. (37) we use classical quadrature formulas of Gaussian type. Let us denote by MD the maximum degree of the polynomials appearing in the integrals, by NPI the number of points of integration and by ED the degree of exactness of the correspondent quadrature formula. In the following table we report the quantities related to the degree p of the finite elements:

Using the number of integration points indicated in Table 3 we compute *exactly* all the integrals appearing in Eq. (37). We remark that the actual computation of the stiffness matrix is made simpler by the fact that the same discrete space is used to approximate displacement and rotation

Table 3 Type of Gaussian integration formulas

p	MD	NPI	ED
1	2	2 × 2	3
2	4	3 × 3	5
3	6	4 × 4	7
4	8	5 × 5	9

components. The quantities are computed and stored once for all and then used to assemble the stiffness matrix. Hereafter we present some results related to the clamped plate problem. The clamped plate is the more effective test to check the robustness of finite elements respect to the locking effect. The reason is due to the fact that a clamped boundary is more prone to locking than a simply supported boundary. For a clamped plate we impose the following condition on the boundary $\partial\Omega$ of the plate

$$w(x,y) = \phi_x(x,y) = \phi_y(x,y)=0 \text{ on } \partial\Omega \tag{38}$$

Several tests with different values of thickness have been performed toanalyse reliability and robustness of finite elements. For each test, among others, displacement at the center C of the plate and the discrete strain energy have been computed. Let $w_{ex}(C)$ denote the exact displacement at the center of the plate (see Timoshenko 1970) and $w_h(C)$ the finite element solution. The relative displacement error is defined as

$$\frac{w_{ex}(C) - w_h(C)}{w_{ex}(C)} \times 100 \tag{39}$$

The exact strain energy was not available. Out of the discrete strain energy an extrapolation has been made in order to get an accurate value of the energy. Let E_{ex} denote such an energy, let E_h be the discrete energy. The relative energy norm $\|e\|$ of the error $e=w_{ex}-w_h$ can be expressed in the following way:

$$\|e\| = \left(\frac{E_{ex} - E_h}{E_{ex}}\right)^{1/2} \times 100 \tag{40}$$

Pointwise evaluation of the displacement error is, of course, a local error indicator whereas the energy norm error is a global indicator. The following figures give the displacement error versus the number of degrees of freedom and the energy norm error versus the reciprocal number of the mesh size parameter. In each figure the dashed line refers to the Serendipity elements, the continuous line to the complete elements, except for the R4 element where only one line is present. We consider a range of values of ratios between thickness and side length varying from t=0.1 (thick plate) to t=0.0001 (very thin plate). In each figure we show the performance of the family of finite elements for a prescribed thickness. Since the numerical results obtained with the elements R15 and R16, R22 and R25, respectively, are very close and the corresponding line overlap in the figures, only the the results for R15 and R22 are reported. We give some comments to the numerical results shown in Figs. 4 to 12.

Let us consider first the displacement error (Figs. 4, 6, 8, 10, 12). In all the figures we can observe that the performance of the complete elements is substantially improved with respect to the Serendipity elements and the locking phenomenon is kept under control, especially when the thickness of the plate becomes smaller. More precisely, for thick plates (t=0.1 and t=0.01 the improvement is less pronounced due to the fact that the corresponding Serendipity elements already give good results. For t=0.001 the improvement is quite remarkable for p=2 and p=3, where the Serendipity elements had poor performances. For t=0.0001 the element R9 and R15 outperform the corresponding Serendipity elements R8 and R12, clearly subject to locking behavior. The element R22, compared with R17, shows very precise results even for coarse decompositions. For very thin plates (t=0.00001) the performance of the elements R15 and R22 is strongly improved with respect to the elements R12 and R17.

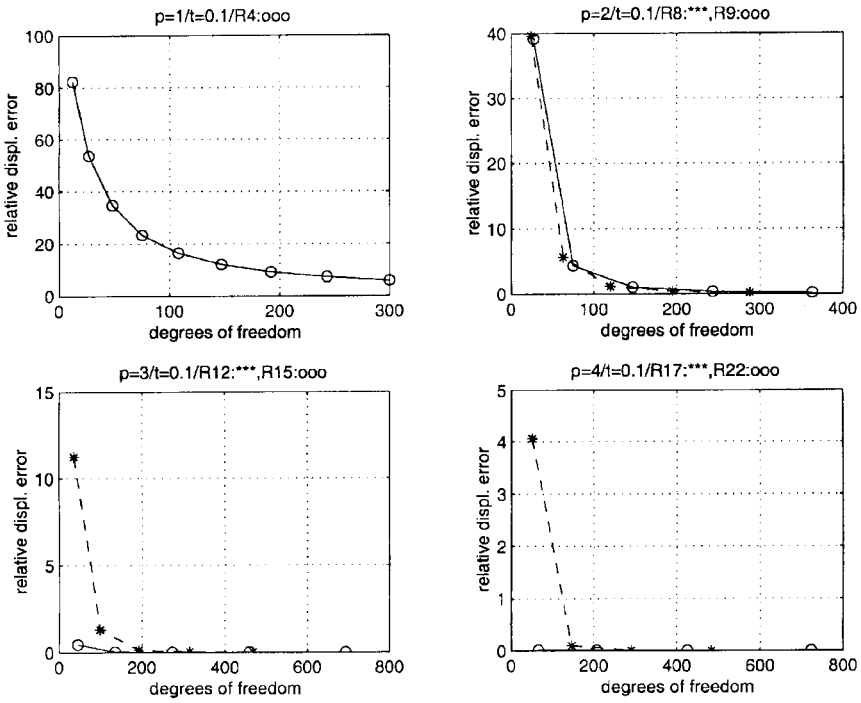

Fig. 4 Relative displacement error vs. d.o.f.; t=0.1; p=1-4

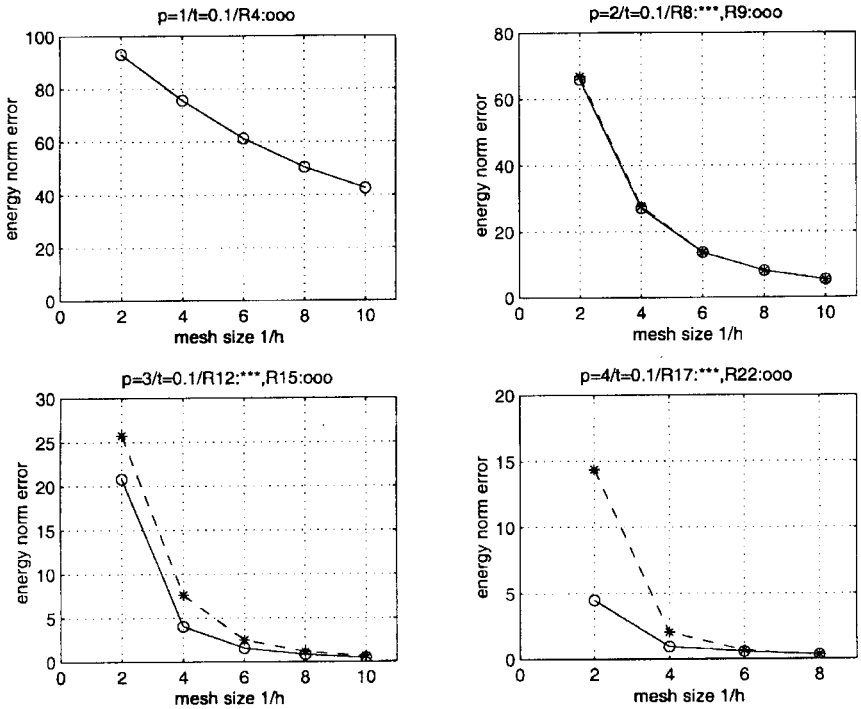

Fig. 5 Energy norm error vs. mesh size; t=0.1; p=1-4

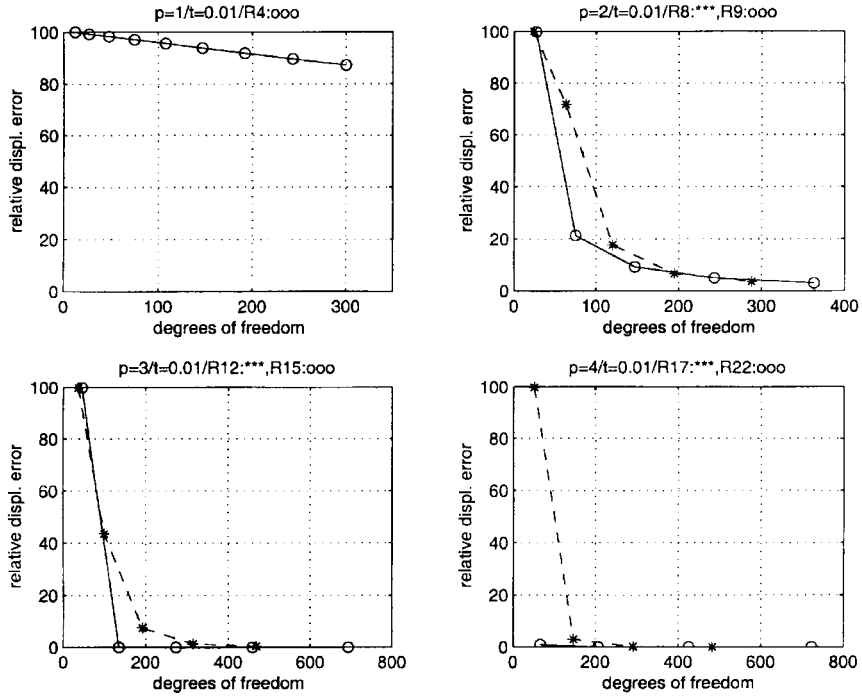

Fig. 6 Relative displacement error vs. d.o.f.; t=0.01; p=1-4

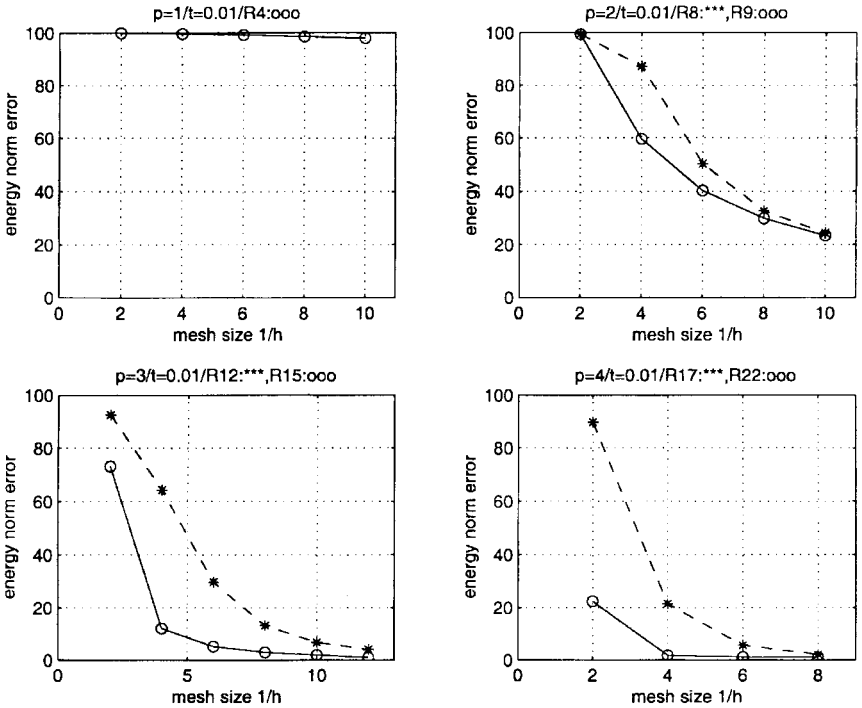

Fig. 7 Energy norm error vs. mesh size; t=0.01; p=1-4

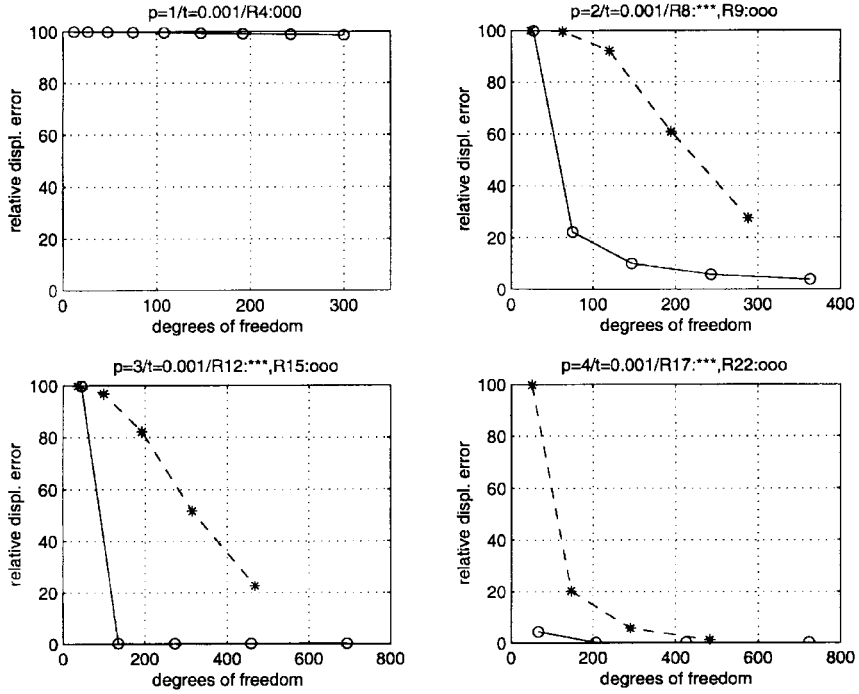

Fig. 8 Relative displacement error vs. d.o.f.; t=0.001; p=1-4

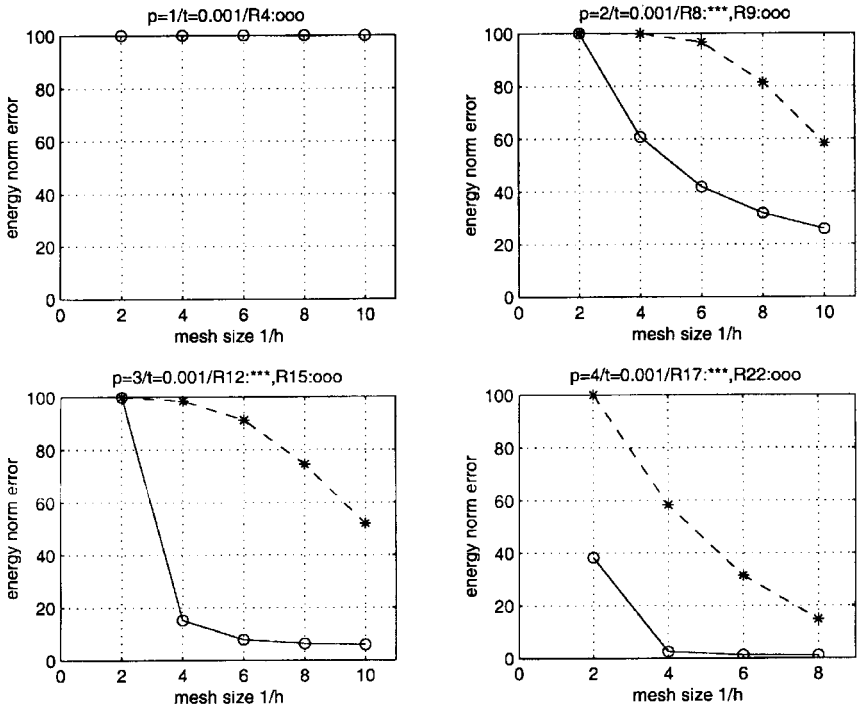

Fig. 9 Energy norm error vs. mesh size; t=0.001; p=1-4

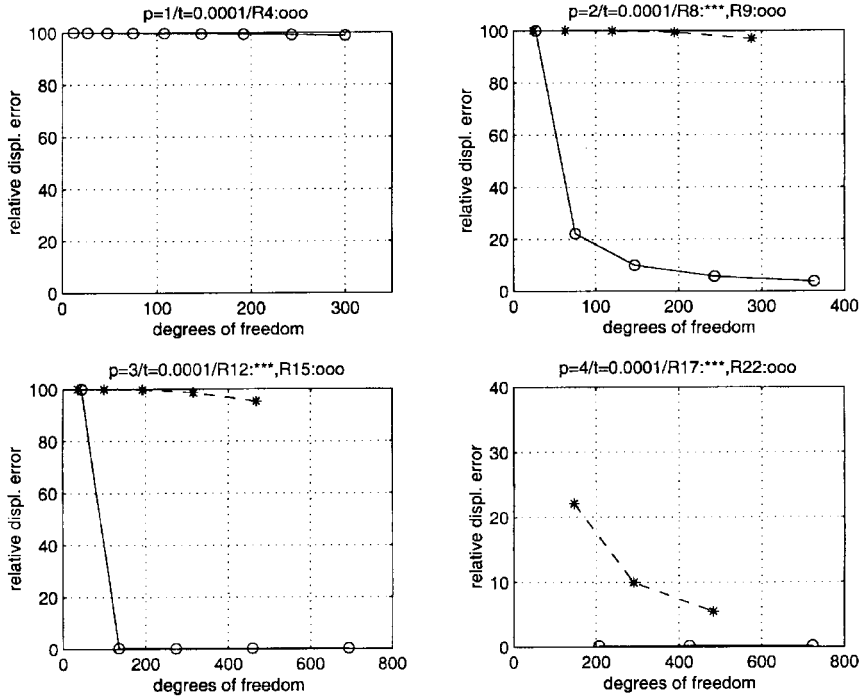

Fig. 10 Relative displacement error vs. d.o.f.; t=0.0001; p=1-4

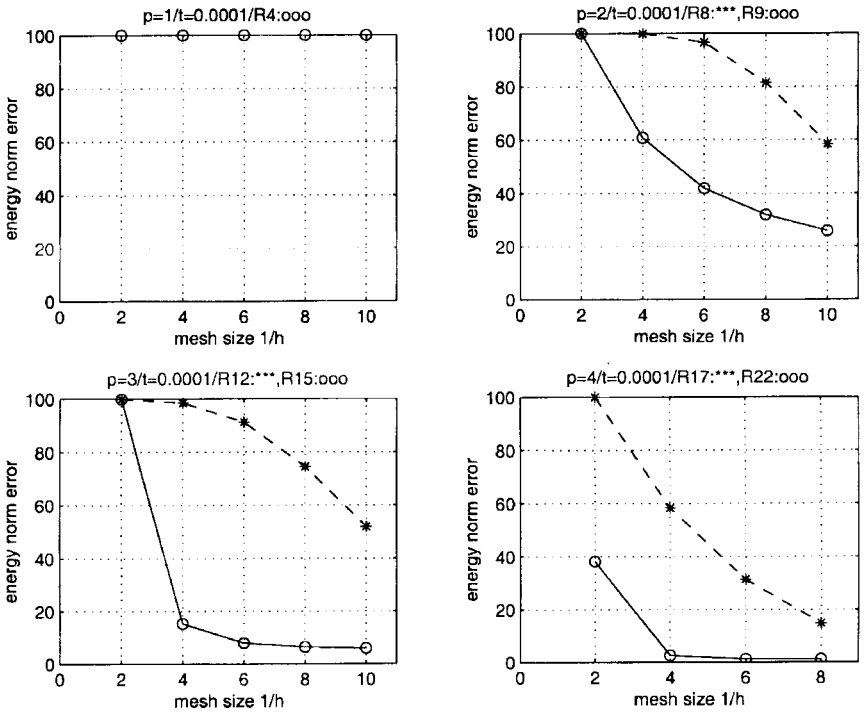

Fig. 11 Energy norm error vs. mesh size; t=0.0001; p=1-4

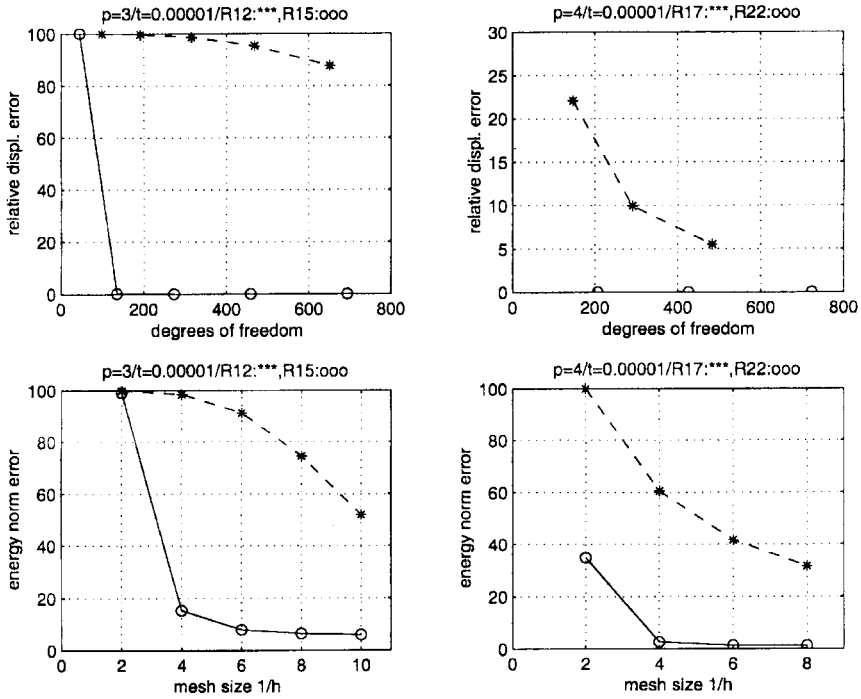

Fig. 12 Relative displacement error vs. d.o.f. and energy norm error vs. mesh size; t=0.00001; p=3-4

Let us now consider the energy norm error (Fig. 5, 7, 9, 11, 12). As we have already pointed out, the energy norm error is a global error indicator. Since no "exact" value of the energy is available. the computation of the energy error is based on an extrapolated value. Following the literature we have computed a value for the "thick" plate (t=0.1) and another value, suitably scaled, for "thin" plates. Such a process, even though not mathematically rigorous, give useful practical hints, since the stabilization of the values of the energy norm error means that the corresponding energy has reached a stable value. The improvement of the performance is unquestionable for all the elements, expecially when thickness becomes smaller. We note that the element R22 is strongly convergent. The other elements all give errors well below the engineering range of accuracy.

6. Conclusions

The numerical results show that the performance of the bubble plus elements is substantially improved with respect to the Serendipity elements and the locking phenomenon is kept under control. The rate of improvement increases as the thickness of the plate becomes smaller. As regards the locking we observe that for p=2 the bubble plus element outperforms the corresponding Serendipity element. For $p \geq 3$ the results show that bubble plus elements strongly reduce the effect of locking. We remark that very close performances are obtained with both the pairs of elements R15, R16 and R22, R25. The cost of the increase of the number of degrees of freedom is negligible compared with the improvement of the results. Therefore, based on our numerical experiences, bubble plus finite elements are more convenient than the corresponding Serendipity elements for

solving Reissner-Mindlin plate problem in its plain formulation.

References

Babuška, I. (1988), "The *p* and *h-p* versions of the finite element method. The state of the art", *Finite Elements: Theory and Application*, D.L. Dwoyer, M.Y. Hussaini, R.G. Voigt (eds), Springer-Verlag, New York, 199-239.

Babuška, I., Elman, H.C. (1993), "Performance of the *h-p* version of the finite element method with various elements", *International J. Numerical Methods in Engineering*, **36**, 2503-2523.

Babuška, I., Scapolla, T. (1989), "Benchmark computation and performance evaluation for a rhombic plate bending problem", *International J. Numerical Methods in Engineering*, **28**, 155-179.

Bathe, K.-J. (1982), *Finite Element Procedures in Engineering Analysis*, Prentice-Hall, Englewood Cliffs, New Jersey

Brezzi, F., Fortin, M. (1991), *Mixed and Hybrid Finite Element Methods*, Springer Verlag, New York.

Ciarlet, P.G. (1978), *The Finite Element Method for Elliptic Problems*, North Holland, Amsterdam.

Della Croce, L., Scapolla, T. (1992), "High order finite elements for thin to moderately thick plates", *Computational Mechanics*, **10**, 263-279.

Della Croce, L., Scapolla, T. (1992), "Hierarchic finite elements with selective and uniform reduced integration for Reissner-Mindlin plates", *Computational Mechanics*, **10**, 121-131.

Della Croce, L., Scapolla, T. (1993), "Transverse shear strain approximation for Reissner-Mindlin plate with high order hierarchic finite elements", *Mechanics Research Communications*, **20**, 1-7.

Della Croce, L., Scapolla, T. (1992), "On the robustness of hierarchic finite elements for Reissner-Mindlin plates", *Computer Methods in Applied Mechanics and Engineering*, **101**, 43-60.

Della Croce, L., Scapolla, T. (1995), "Hierarchic and mixed interpolated finite elements for Reissner-Mindlin plates", *Communications in Numerical Methods in Engineering*, **11**, 549-562.

Della Croce, L., Scapolla, T. (1999a), "Effect of mesh distortion on Serendipity and mixed finite elements solution of thin shells", *International Journal of Applied Science and Computations*, **5**, 220-237.

Della Croce, L., Scapolla, T. (1999b), "Solving cylindrical shell problems with a non-standard finite element", *Mathematics in Computers and Simulation*, in press, **50**, 153-164.

Hughes, T.J.R. (1987), *The Finite Element Method*, Prentice-Hall, Englewood Cliffs, New Jersey.

Perugia, I., Scapolla, T. (1997), "Optimal rectangular MITC finite elements for Reissner-Mindlin plates", *Numerical Methods for Partial Differential Equations*, **13**, 575-585.

Pinsky, P.M., Jasti, R.V. (1989), "A mixed finite element formulation for Reissner-Mindlin plates based on the use of bubble functions", *International J. Numerical Methods in Engineering*, **28**, 1677-1702.

Szabó, B., Babuška, I. (1991), *Finite Element Analysis*, John Wiley & Sons, New York.

Timoshenko, S., Woinowski-Krieger, S. (1970), *Theory of Plates and Shells*, McGraw-Hill, Singapore.

Zienkiewicz, O.C., Taylor, R.L. (1989), *The Finite Element Method*, McGraw-Hill, London, **I**.

Zienkiewicz, O.C., Taylor, R.L. (1991), *The Finite Element Method*, McGraw-Hill, London, **II**.